of the structural units with formation and breaking of moderate intramolecular forces until the contacts and interfaces characteristic of the native state are formed. The results presented here on the refolding of IL-1β would be consistent with this type of mechanism.

References

Brandts, J. F., Halvorson, H., & Brennan, M. (1975) *Biochemistry 14*, 4953-4963.

Buell, G., Schulz, M.-F., Selzer, G., Chollet, A., Movva, N. R., Seman, D., Escanez, S., & Kawashima, E. (1985) *Nucleic Acids Res. 13*, 1923-1938.

Craig, S., Hollecker, M., Creighton, T. E., & Pain, R. H. (1985) *J. Mol. Biol. 185*, 681-687.

Creighton, T. E. (1979) *J. Mol. Biol. 129*, 235-264.

Creighton, T. E., & Pain, R. H. (1980) *J. Mol. Biol. 137*, 431-436.

Dolgikh, D. A., Abaturov, L. V., Bolotina, I. A., Brazhnikov, E. V., Bushuev, V. N., Bychkova, V. E., Gilmanshin, R. I., Lebelev, Y. O., Semestinov, G. V., Tiktopulo, E. I., & Ptitsyn, O. B. (1985) *Eur. Biophys. J. 13*, 109-121.

Donovan, J. W. (1969) in *Physical Principles and Techniques of Protein Chemistry* (Leach, S. J., Ed.) Part A, p 101, Academic, New York.

Duff, G. (1985) *Nature (London) 313*, 352-353.

Feldmann, M. (1985) *Nature (London) 313*, 351-352.

Herskovits, T. T., & Sorensen, M. (1968) *Biochemistry 7*, 2533-2542.

Kim, P. S., & Baldwin, R. L. (1982) *Annu. Rev. Biochem. 51*, 459-489.

Levitt, M., & Chothia, C. (1976) *Nature (London) 261*, 552-558.

March, C. J., Mosley, B., Larsen, A., Cerretti, D. B., Braedt, G., Price, V., Gillis, S., Henney, C. S., Kronheim, S. R., Grabstein, K., Conlon, P. J., Hopp, T. P., & Cosman, D. (1985) *Nature (London) 315*, 641-647.

Mitchinson, C., & Pain, R. H. (1985) *J. Mol. Biol. 184*, 331-342.

Norris, K., Norris, F., Christiansen, L., & Fiil, N. (1983) *Nucleic Acids Res. 11*, 5103-5112.

Provencher, S. W. (1982) *Comput. Phys. Commun. 27*, 229-242.

Provencher, S. W., & Gloeckner, J. (1981) *Biochemistry 20*, 33-37.

Sanger, F., Nicklen, S., & Coulson, A. R. (1977) *Proc. Natl. Acad. Sci. U.S.A. 74*, 5463-5467.

Wallace, R. B., Johnson, P. F., Tanaka, S., Schold, M., Itakura, K., & Abelson, J. (1980) *Science (Washington, D.C.) 209*, 1396-1400.

White, A. (1959) *Biochem. J. 71*, 217-220.

Wingfield, P., Payton, M., Taverneir, J., Barnes, M., Shaw, A., Rose, K., Simona, M. G., Demczuk, S., Williamson, K. W., & Dayer, J. M. (1986) *Eur. J. Biochem. 160*, 491-497.

Wingfield, P., Graber, P., Rose, K., Simona, M. G., & Hughes, G. J. (1987) *J. Chromatogr. 387*, 291-300.

Zoller, M. J., & Smith, M. (1983) *DNA 3*, 479-488.

Comparative Phosphorescence and Optically Detected Magnetic Resonance Studies of Fatty Acid Binding to Serum Albumin†

Su-Yau Mao and August H. Maki*

Department of Chemistry, University of California, Davis, Davis, California 95616

Received November 24, 1986; Revised Manuscript Received February 9, 1987

ABSTRACT: The binding of free fatty acid to bovine serum albumin (BSA) and human serum albumin (HSA) was studied by phosphorescence and optical detection of triplet-state magnetic resonance spectroscopy in zero applied magnetic field. We have found that oleic acid perturbs the excited triplet state of Trp-134 but not that of Trp-212 in BSA. The assignment is made by comparing the BSA results with those obtained from oleic acid binding to HSA. The phosphorescence 0,0 band as well as the zero-field splittings of Trp-134 undergoes significant changes upon binding of oleic acid to BSA. Shifts of the 0,0-band wavelength and of the zero-field splittings point to large changes in the Trp-134 local environment which accompany the complex formation. The shifts are progressive until 3-4 mol of oleic acid is added. The spectroscopic changes may be attributed to Stark effects caused by a protein conformational change near Trp-134 in the BSA–oleate complex. Oleic acid binding has a minimal effect on the triplet-state properties of the single Trp-214 of HSA. The binding specificity with regard to chain length and unsaturation is reflected by the differences in the Trp environment when BSA forms complexes with various fatty acids.

Albumin is the most abundant protein in mammalian plasma. Albumin's most important physiological function is to bind and transport fatty acids, but it also carries many other hydrophobic ligands such as lysolecithin, bilirubin, tryptophan, steroids, and drugs (Goldstein, 1949; Peters, 1975). Serum albumin's structure and function, including fatty acid metabolism and binding sites, have been recently reviewed by Peters (1985). Serum albumin is a single peptide chain of about 580 residues; it is cross-linked by 17 disulfide bonds. The amino acid sequences of bovine serum albumin (BSA)[1] and human serum albumin (HSA) have been compared in some detail by Brown (1977). The general structural details of these are essentially the same; the differences in sequence

† This work was supported by a UC Davis research award to S.-Y.M. and by a research grant to A.H.M. from the National Science Foundation.

[1] Abbreviations: ANS, 1-anilino-8-naphthalenesulfonate; BSA, bovine serum albumin; HSA, human serum albumin; ODMR, optical detection of triplet-state magnetic resonance; SDS, sodium dodecyl sulfate.

0006-2960/87/0426-3576$01.50/0

are generally conservative changes. On the basis of sequence data, analysis of peptide fragments, and hydrodynamic measurements, a three-dimensional model has been developed (Brown & Shockley, 1982). This model contains three major domains, and each domain in turn is comprised of two subdomains, designated as AB and C. Each subdomain consists of a troughlike structure formed by three helices. The inner face of the trough contains predominantly hydrophobic residues. Assembly of two subdomains results in a hydrophobic channel in the center and clusters of basic residues occurring at opposite ends of the domain, which may form electrostatic bonds with the carboxyl group of a fatty acid. The single Trp residue of HSA, Trp-214, lies in subdomain 2-AB, while the two Trp residues of BSA, Trp-134 and Trp-212, are located in subdomains 1-C and 2-AB, respectively.

The binding of fatty acid to serum albumin has been studied extensively. It was concluded that a total of 5–6 mol of long-chain fatty acid bind per mole of albumin with binding constants in the range of 10^7–10^9 M^{-1} and that there are a large number (20–60) of binding sites with lower affinity (Brown & Shockley, 1982). The binding constants of short-chain fatty acids were obtained by equilibrium dialysis and for long-chain fatty acids by partitioning between an organic solvent such as heptane and aqueous albumin solution (Ashbook et al., 1972, 1975). Various spectroscopic studies were also applied to investigate the structural and binding properties of albumin. The absorption and fluorescence spectra of conjugated polyene long-chain fatty acids were used to study their binding to BSA (Sklar et al., 1977) and to HSA (Berde et al., 1979). Proximity relationships were determined by energy transfer between albumin's Trp residues and the polyene chromophore. In addition, several nitroxide-labeled fatty acids have been used to elucidate binding geometries (Morrisett et al., 1975; Ruf & Gratzl, 1976; Berde et al., 1979). Furthermore, the fluorescence of Trp residues in albumin has been useful for studying the mechanism of fatty acid interaction with proteins and has led to a hypothesis about localization of the Trp residues in the fatty acid binding sites (Spector, 1975). In BSA, only one of the Trp residues is thought to reside near a site of high affinity, but there remains some uncertainty concerning the identity of the Trp.

Here, we present the application of optical detection of triplet-state magnetic resonance (ODMR) spectroscopy to the investigation of serum albumin binding to naturally occurring fatty acids. ODMR spectroscopy has been applied to study protein structure for more than a decade (Kwiram, 1982; Maki, 1984). In the ODMR technique, the phosphorescence of a triplet chromophore is observed while the microwave frequency transitions are induced between the magnetic sublevels of the triplet state. It has been used to probe the local environment of aromatic amino acid residues, of which Trp has been the most extensively studied. The zero-field splittings are sensitive to local electric fields (Stark shifts) (von Schütz et al., 1974; van Egmond et al., 1975) and thus can serve to monitor changes which occur in the environment. In particular, the trends in triplet-state properties of Trp vs. local polarity and polarizability have been summarized by Hershberger et al. (1980). BSA is among the proteins first studied by ODMR spectroscopy (Zuclich et al., 1972), and ODMR studies of HSA have been carried out recently by Bell and Brenner (1982).

In this paper, we report phosphorescence and ODMR measurements on BSA and HSA as the proteins are bound to fatty acids. Large shifts in phosphorescence 0,0-band and zero-field splittings which occur upon oleic acid complexing with BSA are attributed to one of the Trp residues near a primary binding site. By comparing the results of BSA and HSA, we find that the changes in the BSA phosphorescence and ODMR spectra upon oleate binding are due to Trp-134, and they are consistent with the location of this residue in a polar region.

For the purpose of comparison, the binding of stearic acid and octanoic acid to albumins also is investigated.

Materials and Methods

Bovine serum albumin (BSA) and human serum albumin (HSA), crystallized, lyophilized, and essentially fatty acid free (less than 0.005%), were obtained from Sigma and were used without further purification. SDS–polyacrylamide (15%) gel electrophoresis indicated the albumins are free of impurities (less than 2%) as determined by Coomassie Brilliant Blue staining. The content of albumin dimers and higher oligomers in equilibrium with monomers has been discussed by Morrisett et al. (1975), where it was reported not to affect fatty acid binding. Protein concentrations were determined from the absorbance at 279 nm by using $E^{1\%}_{1cm} = 6.67$ for BSA (Janatova et al., 1968) and 5.31 for HSA (Edwards et al., 1969). Solutions of BSA and HSA (ca. 5×10^{-4} M) were prepared in 50 mM sodium phosphate buffer, pH 7.4. For low-temperature spectroscopic measurements, 20% (v/v) glycerol (Aldrich Gold Label) was added. Doubly distilled water and solvents of spectroscopic grade were used throughout the experiments. All other chemicals were of the purest quality available. Oleic acid, stearic acid, and octanoic acid were obtained from Aldrich. Ethanolic solutions of the fatty acids were used for addition to aqueous albumin solutions in the binding experiments. The final ethanol concentration in the solutions did not exceed 2% and had no effect on the measurements.

Samples were contained in quartz tubes which were inserted into a microwave slow-wave helix terminating a coaxial transmission line. This was then suspended in a Dewar and chilled to 1.2 K by pumping on the liquid helium. the sample was excited with a 100-W high-pressure Hg arc equipped with a 12-cm path-length aqueous $NiSO_4$ (500 g/L) infrared filter. The excitation band centered at 295 nm was selected with a monochromator using 4-nm bandwidth to prevent tyrosine excitation. The phosphorescence at a right angle to the excitation path passed through a WG-345-2 glass filter and was collected by a 600 groove/mm 1-m monochromator (McPherson Model 2051) and detected by a cooled photomultiplier tube (EMI Model 9789QA). Data analysis was carried out on a Digital PRO-350 microcomputer interfaced to a 1024-channel signal averager (Nicolet Model 1072).

The phosphorescence spectra were recorded with a 1.5-nm bandwidth at 4.2 K, and the 0,0 band was monitored at its peak wavelength by using a 3-nm bandwidth for ODMR measurements. Microwaves were swept both with increasing and with decreasing frequency at the same rate of 30 MHz/s, and the peak frequencies were averaged to obtain the zero-field splittings. The swept frequencies were calibrated by a microwave frequency counter (Hewlett Packard Model 5351A). Wavelength-selected ODMR measurements were performed with a bandwidth of 1.0 or 1.2 nm.

Results

Phosphorescence Spectroscopy. The phosphorescence spectra of BSA and the BSA–oleate complex are compared in Figure 1. The 0,0 band of BSA occurs at 413.7 nm, which is close to that found for Trp in a hydrophobic environment. Upon addition of oleic acid, a new band appears at 406.1 nm, and the intensity of this band increases progressively until 3–4

Table I: Comparison of Triplet-State Parameters for BSA, HSA, and Complexes Formed between Albumins and Various Fatty Acids

	$\lambda_{0,0}$ (nm)	ν_1 ($\Delta\nu$)[a]	ν_2 ($\Delta\nu$)[a]	D (GHz)	E (GHz)
BSA	413.7	1.649 (123)	2.572 (215)	2.935	1.286
HSA	412.6	1.684 (146)	2.539 (228)	2.953	1.269
BSA + oleate (1:4)	406.1	1.807 (118)	2.386 (197)	3.001	1.193
	414.1	1.650 (–)[b]	2.570 (–)[b]	2.935	1.285
BSA + stearate (1:4)	413.1	1.683 (143)	2.524 (231)	2.945	1.262
BSA + octanoate (1:20)	406.1	1.816 (140)	2.344 (259)	2.988	1.172
	412.3	1.693 (155)	2.560 (253)	2.973	1.280
BSA + octanoate (1:50)	410.7	1.715 (143)	2.522 (281)	2.976	1.261
HSA + oleate (1:20)	411.9	1.698 (139)	2.518 (230)	2.957	1.259
HSA + octanoate (1:20)	412.1	1.689 (122)	2.531 (225)	2.955	1.265

[a] Peak ODMR frequencies in gigahertz; the values given are the average of frequencies observed sweeping in both directions. The numbers in parentheses are line widths (full width at half-maximum) in megahertz. [b] The line widths were not measured.

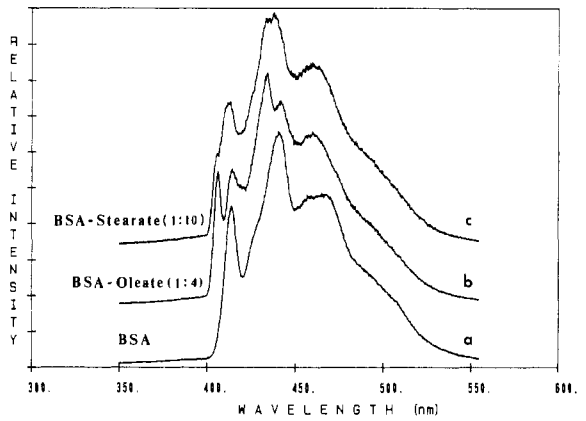

FIGURE 1: Phosphorescence spectra at 4.2 K of (a) BSA, (b) BSA + oleic acid (1:4), and (c) BSA + stearic acid (1:10). The solvent is 20% (v/v) glycerol/aqueous 50 mM phosphate buffer, pH 7.4. BSA concentration is ca. 5×10^{-4} M.

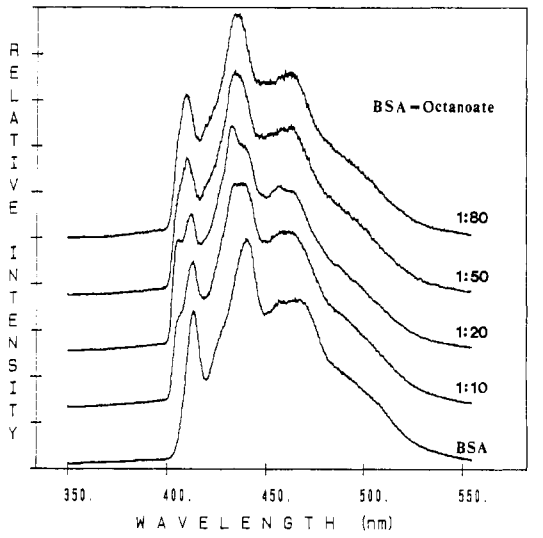

FIGURE 2: Phosphorescence spectra at 4.2 K of BSA–octanoate complexes with various molar ratios.

mol of fatty acid is added, while the second peak undergoes only a small shift from 412.9 to 414.1 nm. The newly occurring band is significantly narrower than the 0,0 band of BSA, suggesting a decrease in the heterogeneity of the microenvironment upon complex formation, and the peak wavelength is consistent with Trp in a polar environment. These results indicate that upon binding to oleic acid, only one Trp residue of BSA becomes greatly perturbed and no longer has an environment comparable to the other; therefore, the 0,0 bands originating from individual Trp residues become resolved. This is indicative of the presence of one Trp residue in the vicinity of a high-affinity binding site for oleic acid.

To identify the Trp residue involved in oleate binding, the same measurements were carried out for HSA. The 0,0 band of the lone Trp in HSA peaks at 412.6 nm and is somewhat less resolved than that of BSA. Binding of oleic acid to HSA up to an oleate:albumin ratio of 20 has essentially no effect on the Trp phosphorescence spectrum, suggesting that the binding sites are not near the single Trp residue of HSA.

It was of interest to study serum albumin binding to a long-chain saturated fatty acid and to compare the results with those obtained from the binding of oleic acid, which contains a cis double bond between carbon atoms 9 and 10. Therefore, stearic acid, also 18 carbons in length, was used to investigate the possible effect of substrate geometry on binding. Figure 1 shows the phosphorescence spectrum of the BSA–stearate complex compared with that of BSA. Both Trp residues are blue-shifted by stearic acid, and their 0,0 bands are not well resolved.

It has been shown that short-chain fatty acids through decanoate bind at different sites than the longer chain fatty acids (Koh & Means, 1979). In this study, octanoic acid was used to investigate short-chain fatty acid binding to albumins. It did not perturb the phosphorescence spectrum of the lone Trp residue of HSA until a large excess (albumin:octanoate molar ratio = 1:20) was added. The 0,0 band shifted slightly from 412.6 to 412.1 nm and is somewhat better resolved than that of HSA. The changes in the phosphorescence spectrum of BSA upon complexing with octanoate are more complicated (Figure 2). At an octanoate:albumin ratio of 10, a shoulder appears at the blue of the 0,0 band of BSA and becomes more pronounced at a ratio of 20, where it peaks at 406.1 nm. this new band is similar to the 0,0 band of the perturbed Trp in the BSA–oleate complex, but it is less intense. The remaining 0,0 band is shifted slightly, and the wavelength maximum is close to that of the HSA complex with octanote at an octanoate:albumin ratio of 20. This band is blue-shifted further at higher octanoate concentration, and it finally becomes overlapped with the 406.1-nm band.

ODMR Spectroscopy. Table I lists the ODMR signals for BSA, HSA, and the complexes formed between these albumins and fatty acids. The zero-field splittings of BSA, ν_1 = 1.649 GHz, ν_2 = 2.572 GHz, together with the line widths are similar to those for Trp located in a buried and hydrophobic protein environment, whereas the ODMR signals of HSA suggest that the lone Trp residue is not fully protected from the solvent. When BSA is complexed with oleic acid at a molar ratio of 1 to 4, the ODMR transitions monitored at the 0,0 band of the perturbed Trp (406.1 nm) are quite different from those of BSA. The $|D|-|E|$ transition increases by 158 MHz to 1.807 GHz, while the $2|E|$ frequency is reduced by 186 MHz to 2.386 GHz (Figure 3). These frequencies and the 0,0-band wavelength suggest that the perturbed Trp is located in a polar region. However, the narrow line widths of the 0,0 band and

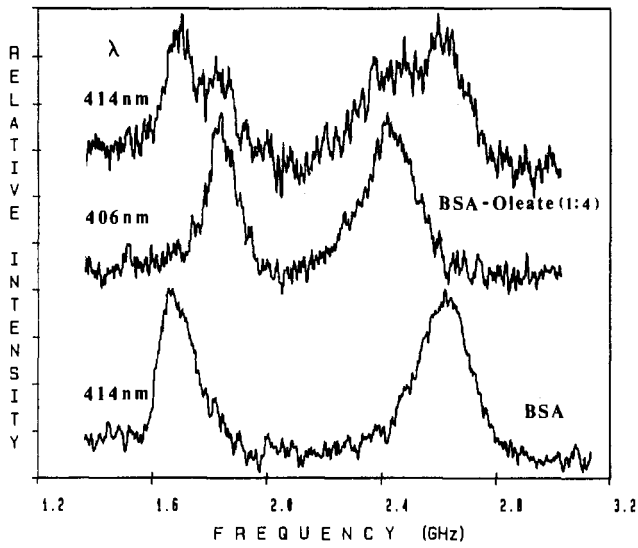

FIGURE 3: $|D|-|E|$ (low-frequency) and $2|E|$ (high-frequency) ODMR transitions of BSA and BSA–oleate (1:4) complex. The wavelength shown is the peak wavelength of the individual 0,0 band monitored. The samples are prepared in the solution described in the caption of Figure 1. Signal-averaged spectra (ca. 60 repetitions) shown are made with microwaves scanned up in frequency from 1.4 to 3.0 GHz at a rate of 30 MHz/s.

the ODMR signals indicate that the polar site is in the interior of the protein (Hershberger et al., 1980). When monitored at the second peak, 414.1 nm, the zero-field splittings are essentially the same as those of BSA. The spectra have some contribution from a vibronic band of the blue-shifted site, whose wavelength coincides with the red-shifted 0,0 band. For stearic acid binding to BSA at a stearate:albumin ratio of 4, the ODMR signals undergo only small shifts; i.e., the $|D|-|E|$ frequency increases by 34 MHz, and the $2|E|$ frequency is reduced by 48 MHz. This is very different from the results using oleic acid, suggesting that unsaturation has a significant effect on the binding.

It has been shown above that octanoic acid binding does not perturb either Trp residue of BSA until a high fatty acid to albumin ratio is reached. At a molar ratio of 20, however, the $|D|-|E|$ transition occurs at a high frequency, 1.816 GHz, and the $2|E|$ signal appears at 2.344 GHz when monitored at the blue 406.1-nm 0,0 band. These frequencies are similar to those of the perturbed Trp in the BSA complex with oleic acid, although the line widths of the ODMR signals are considerably larger in the BSA–octanoate complex. As for the ODMR transitions monitored at the 412.3-nm peak, the frequencies are comparable to those measured at the 0,0 band (412.1 nm) of the HSA–octanoate complex. These results indicate that the primary binding sites for octanoic acid are not near either Trp residue in these albumins; when the primary sites are occupied, the excess fatty acid appears to spill over and only then begins to occupy sites in the vicinity of Trp residues.

Wavelength-Selected ODMR. The occurrence of discontinuities in the zero-field splittings with changing observed phosphorescence wavelength may be indicative of emission from distinct Trp sites in the protein (von Schütz, 1974). This will be the case only for discontinuities observed by monitoring phosphorescence within the 0,0 band of the tryptophan phosphorescence spectrum. Kwiram et al. (1978) have shown, for instance, that for a single tryptophan site, a discontinuity is observed as the emission is tracked between the 0,0 band and the first vibronic band. In this study of wavelength-selected ODMR, we were careful to remain within the 0,0-band

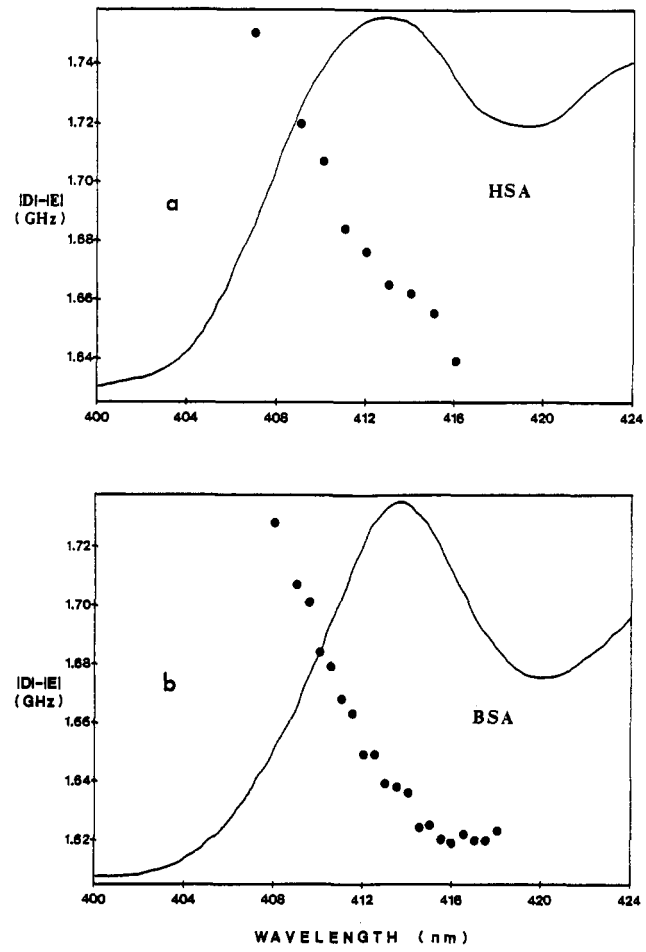

FIGURE 4: Variation in the $|D|-|E|$ zero-field transition frequency as a function of emission wavelength for (a) HSA and (b) BSA. Serum albumin concentration is ca. 10^{-3} M. The slit resolution is 1.2 nm for HSA and 1.0 nm for BSA. The $|D|-|E|$ transition was measured with microwaves scanned up in frequency from 1.4 to 2.0 GHz at a rate of 17 MHz/s. The difference in $|D|-|E|$ for sweeps made at this rate toward lower frequency is on the average 36 MHz; the values shown in the graph have been corrected by subtracting 18 MHz from the measured frequencies. The phosphorescence 0,0 band is shown for reference.

region of tryptophan phosphorescence using a narrow bandwidth (1.0 or 1.2 nm). In Figure 4a, the $|D|-|E|$ transition frequencies of HSA are plotted vs. wavelength. A single set of signals is observed, whose frequencies vary monotonically and approximately linearly with wavelength. Figure 4b shows the variation in the $|D|-|E|$ frequency with observing wavelength for BSA. A change in slope occurs at ca. 414 nm and separates the signals into two sets, indicating that they originate from distinct Trp sites. The first set of signals varies linearly with wavelength, and the dependence is similar to that of HSA, whereas the second set of signals is wavelength independent and is found in the red-shifted part of the 0,0 band. In order to get further evidence for the Trp perturbation in fatty acid binding, wavelength-selected ODMR was also carried out for the complexes formed between albumins and fatty acids. As shown in Figure 5 (curve c), the wavelength-independent set of signals of BSA (curve a) have disappeared in the BSA–oleate (1:4) complex, while a new set of signals appears at higher frequencies when monitored throughout the blue-shifted 0,0 band (Figure 1b). The low-frequency region of the BSA–oleate complex resembles that of HSA (Figure 5b), indicating that the common Trp is not perturbed by oleate binding, while the binding site containing Trp-134 undergoes a dramatic change upon complexing with

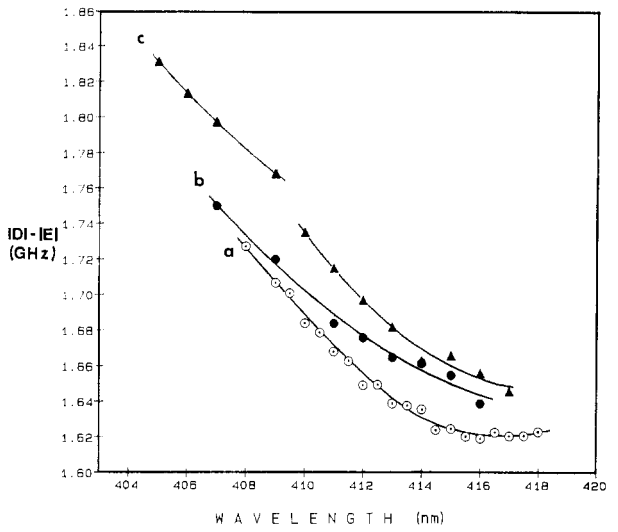

FIGURE 5: Wavelength dependence of the $|D|-|E|$ zero-field transition frequency of the BSA–oleate complex compared with those of BSA and HSA. (a) BSA (⊙), (b) HSA (●), (c) BSA–oleate (1:4) complex (▲). BSA concentration was ca. 5×10^{-4} M in the BSA–oleate complex, and a slit resolution of 1.0 nm was used for the measurements of this sample.

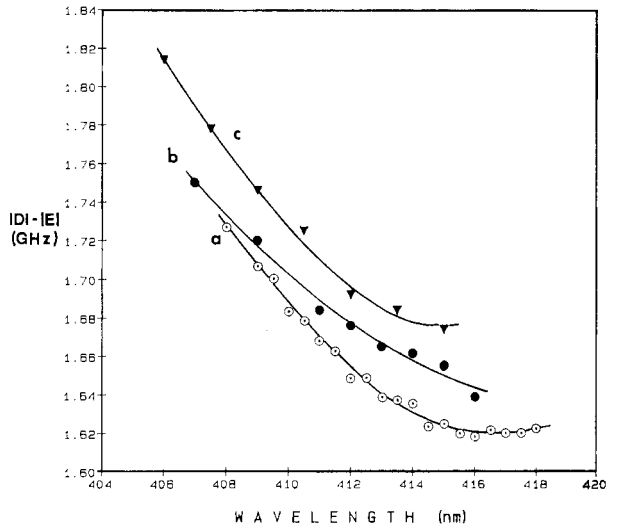

FIGURE 6: Wavelength dependence of the $|D|-|E|$ zero-field transition frequency of the BSA–octanoate complex compared with those of BSA and HSA. (a) BSA (⊙), (b) HSA (●), (c) BSA–octanoate (1:56) complex (▼). BSA concentration was ca. 5×10^{-4} M in the BSA–octanoate complex, and a slit resolution of 1.2 nm was used.

oleate. Figure 6 shows the wavelength dependence of $|D|-|E|$ signals for the BSA–octanoate complex (1:56) in comparison with those of uncomplexed BSA and HSA. Both Trp-134 and Trp-212 of BSA are perturbed in the complex.

Discussion

The microenvironment of the lone Trp residue of HSA has been characterized by various spectroscopic studies. Bell and Brenner (1982) have found that the phosphorescence 0,0-band maximum and $|D|-|E|$ zero-field splitting frequency are consistent with the location of Trp-214 in a hydrophobic region. However, the Trp fluorescence is quenched by iodide ions (Fuller Noel & Hunter, 1972) and ANS (Santos & Spector, 1974). Moreover, a neutral quencher, acrylamide, is able to quench the fluorescence of the Trp residue with a surprisingly large rate constant (Eftink & Ghiron, 1977). The argument was made that in order for collision between quencher and the buried indole ring to occur, fluctuations in the protein matrix must facilitate the inward movement of the quencher. Therefore, it was concluded that the Trp residue in HSA is surrounded by layers of an amorphous and permeable protein matrix. This agrees with the results obtained in the present study. The phosphorescence 0,0-band and ODMR signals are quite broad, indicating a rather heterogeneous environment for Trp-214 although it is buried in the protein interior.

The situation is more complex in BSA because it contains two Trp residues, Trp-134 and Trp-212. The phosphorescence 0,0 band appears as a single peak with a red-shifted wavelength maximum. The zero-field splittings and ODMR line widths are also consistent with Trp buried in a hydrophobic region of protein. von Schütz et al. (1974) were able to distinguish between several emissive Trp residues whose 0,0 bands were not resolved by systematically measuring the ODMR splittings as a function of wavelength across the phosphorescence spectrum. They found abrupt breaks in the value of the zero-field splittings or in the slope of the zero-field splittings vs. wavelength curve. These discontinuities were interpreted as arising from different Trp residues in the protein. Thus, even though the optical spectrum of BSA provides no resolution of emission from individual residues, this approach enables us to distinguish between Trp residues more effectively. The dependence of $|D|-|E|$ transition on wavelength shows a break in the slope in the region of the overlapping 0,0 bands; a systematic reduction in the $|D|-|E|$ frequency with increasing wavelength occurs throughout the blue region but levels off toward the red edge of the 0,0 band. The wavelength dependence in the blue region is very similar to that shown by HSA; the blue-shifted emission of BSA probably originates from the common Trp residue. Therefore, the red edge of the BSA 0,0 band and the wavelength-independent $|D|-|E|$ transitions may be attributed to Trp-134 in BSA. According to the trends found by Hershberger et al. (1980), Trp-134 is located inside the globular structure in a hydrophobic and relatively homogeneous environment.

A related study which differentiates individual Trp residues in BSA used fluorescence quenching by iodide ions and was carried out on bovine mercaptalbumin and non-mercaptalbumin (Fuller Noel & Hunter, 1972). It is known that the sulfhydryl titer of BSA samples is invariably fractional, typically about 0.6–0.7 mol/mol (Hughes, 1947; Simpson & Saroff, 1958); the term mercaptalbumin refers to the fraction having a freely reactive sulfhydryl group and non-mercaptalbumin to the fraction showing no sulfhydryl reactivity. Fluorescence quenching results showed that only one Trp residue is available to iodide, and this quenchable Trp exhibits the same fluorescence behavior regardless of the sulfhydryl content of these proteins. However, the fluorescence of the unquenched Trp is greatly decreased in the case of the non-mercaptalbumin. It was postulated that the unquenched Trp is in the vicinity of the mercaptalbumin sulfhydryl group. According to the amino acid sequence data (Brown & Shockley, 1982), the single cysteine, Cys-34, is located in domain 1. Thus, the identity of the unquenched Trp is more likely to be Trp-134. Furthermore, these authors also carried out experiments on HSA and found that its lone Trp residue was quenched in a manner very similar to that of the quenchable Trp of the bovine protein. Therefore, Trp-214 in HSA is in an environment which approximates that of the quenchable Trp residue of BSA, Trp-212. Although human and bovine serum albumins are not strictly equivalent, i.e., fatty acids bind more tightly to BSA than HSA (Spector & Fletcher, 1978), the following comparison was made with the assumption that the fatty acid binding sites on these proteins are homologous.

When oleic acid, a long-chain fatty acid, binds to BSA, the overlapping phosphorescence 0,0 bands split and move in opposite directions. This is mainly due to the perturbation of one 0,0-band origin, producing a large blue-shift so that the individual Trp residues become optically resolved. The changes are progressive until 3–4 mol of oleate is added. The blue band peaks at 406 nm, while the red band peaks at 414 nm. Variation in the local environment of Trp residues is also reflected in the zero-field splittings. When monitoring at 406 nm, we observed large shifts in transition frequencies as well as a reduction in line widths, indicating one Trp is now located in a polar but relatively homogeneous environment; i.e., it is not exposed to the solvent, whereas the Trp corresponding to 414 nm is in a hydrophobic region. On the contrary, oleic acid binding has little effect on the lone Trp in HSA. To identify the Trp which becomes greatly perturbed upon oleate binding, wavelength-selected ODMR was carried out on the BSA–oleate complex with molar ratio 1:4, where the changes both in phosphorescence and in zero-field splittings have saturated. The wavelength dependence of $|D|-|E|$ for the 414-nm band is surprisingly close to that of HSA and is distinct from the dependence of the 406-nm band. It is significant that the wavelength-independent curve of Trp-134 in BSA has vanished in the complex and is replaced by a new set of wavelength-dependent signals at shorter wavelength.

These results suggest that Trp-134 in BSA is located near one of the primary binding sites for the long-chain fatty acid and becomes greatly perturbed upon oleate binding. The nature of the Trp-134 local environment in the complex is polar and relatively homogeneous, rather than being hydrophobic. Therefore, the alkyl chain of oleic acid bound at this site does not interact directly with the Trp residue. The perturbation of Trp-134 may be due to interaction with the polar head of the fatty acid or to a progressive protein conformational change induced by oleate binding. The binding has a minimal effect on the other Trp residue of BSA, Trp-212, or on the lone Trp-214 in HSA.

Spector and John (1968) found that the average fluorescence quantum yield of the tryptophans of BSA decreases as oleic acid binds to the protein. A similar decrease in emission intensity is observed with the binding of most long-chain fatty acids and is accompanied by a relatively small blue-shift (<7 nm) in the Trp fluorescence spectrum. This decrease in quantum yield is not due to energy transfer but rather to a conformational effect that changes the excited singlet-state decay rate (Sklar et al., 1977). Furthermore, the maximum reduction in fluorescence intensity never exceeded 45%. The following explanation has been proposed by Spector (1975) to account for these fluorescence intensity and wavelength changes. One of the tryptophans of BSA is located deep inside the globular structure, whereas the other is superficially located and fairly accessible to solvent. Several of the strong fatty acid binding sites are located within 10 Å of the buried tryptophan residue, but the alkyl chains bound at these sites do not interact directly with the Trp residue. The configurational adaptability (Karush, 1950, 1954) that accompanies fatty acid binding to these sites alters the environment of this buried Trp residue, leading to progressive quenching of the fluorescence as the strong binding sites are filled. The blue-shift in the fluorescence spectrum results from movement of the second, or superficial, Trp residue into an environment that is more protected from the solvent. This change is also progressive and, hence, secondary to structural changes associated with fatty acid binding at other locations in the albumin molecule. Our results are in agreement with this hypothesis, as well as with the structural model proposed by Brown and Shockley (1982), where subdomain 1-C was postulated as one of the primary binding sites for long-chain fatty acids.

It seems likely that the binding sites, which prefer long-chain fatty acids, show some specificity with regard to chain length and unsaturation. Spector and Fletcher (1978) have found that the strength of binding increases as the length of the alkyl chain increases (lauric < palmitic < stearic), suggesting that the main energy of binding is due to hydrophobic interactions. At a given chain length, the insertion of a single cis double bond increases the strength of binding (oleate > stearate). This is indicative that binding depends on the structure of the fatty acid hydrocarbon chain. In contrast to strong Trp perturbation resulting from oleate binding, stearate binding to BSA induces relatively small changes in the phosphorescence and zero-field splittings of Trp. This may be attributed to differences in the configurational geometry of these fatty acids. The cis double bond in oleic acid produces a rigid bend in the aliphatic chain, while stearic acid has the freedom of rotation around its single bonds and thus is more flexible and elongated. Differences in binding affinities due to some variation in the configurational geometry of the hydrocarbon chain would be expected. Moreover, these fatty acid molecules are likely to have different orientations when they bind to albumins and thus induce different conformational changes in the vicinity of Trp residue, which would account for the observations in the present study.

As for the binding of octanoic acid to both BSA and HSA, our results show that none of the Trp residues are perturbed until a large excess of fatty acid has been added. Therefore, the primary binding sites for short-chain fatty acid are not located near either Trp. A specific binding site for short-chain fatty acids up to decanoate has been determined by Koh and Means (1979) using inhibition of the acetylation of Tyr-411 of HSA by nitrophenyl acetate. This high-affinity binding site corresponds to subdomain 3-AB in the structural model proposed by Brown and Shockley (1982). Binding of octanoic acid at this site is thus too distant to affect the environment of either Trp residue in these albumins.

In this study, we have demonstrated that ODMR spectroscopy is useful in elucidating the structural and binding properties of serum albumins complexing with fatty acids, and we have been able to characterize the role of distinct subdomains containing Trp residues in the binding.

Registry No. Oleic acid, 112-80-1; stearic acid, 57-11-4; octanoic acid, 124-07-2; tryptophan, 73-22-3.

References

Ashbook, J. D., Spector, A. A., & Fletcher, J. E. (1972) *J. Biol. Chem. 247*, 7030–7042.

Ashbook, J. D., Spector, A. A., Santos, E. C., & Fletcher, J. E. (1975) *J. Biol. Chem. 250*, 2333–2338.

Bell, K. L., & Brenner, H. C. (1982) *Biochemistry 21*, 799–804.

Berde, C. B., Hudson, B. S., Simoni, R. D., & Sklar, L. A. (1979) *J. Biol. Chem. 254*, 391–400.

Brown, J. R. (1977) in *Albumin: Structure, Function, and Uses* (Rosenoer, V. M., Oratz, M., & Rothschild, M. A., Eds.) pp 27–51, Pergamon Press, Oxford.

Brown, J. R., & Shockley, P. (1982) in *Lipid–Protein Interactions* (Jost, P. C., & Griffith, O. H., Eds.) Vol. 1, pp 25–68, Wiley, New York.

Edelhoch, H. (1967) *Biochemistry 6*, 1948–1954.

Edwards, F. B., Rombauer, R. B., & Campbell, B. J. (1969) *Biochim. Biophys. Acta 194*, 234–245.

Eftink, M. R., & Ghiron, C. A. (1977) *Biochemistry 16*, 5546–5551.

Fuller Noel, J. K., & Hunter, M. J. (1972) *J. Biol. Chem. 247*, 7391–7406.
Goldstein, A. (1949) *Pharmacol. Rev. 1*, 102–165.
Hershberger, M. V., Maki, A. H., & Galley, W. C. (1980) *Biochemistry 19*, 2204–2209.
Hughes, W. L., Jr. (1947) *J. Am. Chem. Soc. 69*, 1836–1837.
Janatova, J., Fuller, J. K., & Hunter, M. J. (1968) *J. Biol. Chem. 243*, 3612–3622.
Karush, R. (1950) *J. Am. Chem. Soc. 72*, 2705–2713.
Karush, R. (1954) *J. Am. Chem. Soc. 76*, 5536–5542.
Koh, S.-W. M., & Means, G. E. (1979) *Arch. Biochem. Biophys. 192*, 73–79.
Kwiram, A. L. (1982) in *Triplet State ODMR Spectroscopy* (Clark, R. H., Ed.) pp 427–478, Wiley, New York.
Kwiram, A. L., Ross, J., B. A., & Deranleau, D. A. (1978) *Chem. Phys. Lett. 54*, 506–509.
Maki, A. H. (1984) in *Biological Magnetic Resonance* (Berliner, L. J., & Reuben, J., Eds.) pp 187–294, Plenum Press, New York.
Morrisett, J. D., Pownall, J. H., & Gotto, A. M. (1975) *J. Biol. Chem. 250*, 2487–2494.
Peters, T. (1975) in *The Plasma Proteins* (Putnam, F. W., Ed.) Vol. 1, pp 133–181, Academic Press, New York.
Peters, T. (1985) *Adv. Protein Chem. 37*, 161–245.
Ruf, H. H., & Gratzl, M. (1976) *Biochim. Biophys. Acta 446*, 134–142.
Santos, E. C., & Spector, A. A. (1974) *Mol. Pharmacol. 10*, 519–528.
Simpson, R. B., & Saroff, H. A. (1958) *J. Am. Chem. Soc. 80*, 2129–2131.
Sklar, L. A., Hudson, B. S., & Simoni, R. D. (1977) *Biochemistry 16*, 5100–5108.
Spector, A. A. (1975) *J. Lipid Res. 16*, 165–179.
Spector, A. A., & John, K. M. (1968) *Arch. Biochem. Biophys. 127*, 65–71.
Spector, A. A., & Fletcher, J. E. (1978) in *Disturbances in Lipid and Lipoprotein Metabolism* (Dietschy, J. M., Gotto, A. M., & Ontko, J. A., Eds.) pp 229–249, Waverly, Baltimore.
van Egmond, J., Kohler, B. E., & Chan, I. Y. (1975) *Chem. Phys. Lett. 34*, 423–426.
von Schütz, J. U., Zuclich, J., & Maki, A. H. (1974) *J. Am. Chem. Soc. 96*, 714–718.
Zuclich, J., Schweitzer, D., & Maki, A. H. (1972) *Biochem. Biophys. Res. Commun. 46*, 1764–1768.

Functional, Chymotryptically Split Actin and Its Interaction with Myosin Subfragment 1†

Kunihiko Konno‡
Cardiovascular Research Institute, University of California, San Francisco, San Francisco, California 94143
Received June 2, 1986; Revised Manuscript Received January 30, 1987

ABSTRACT: We have prepared chymotryptically split actin that retains the characteristic properties of intact actin. Chymotryptic digestion of G-actin produces an intermediate 35-kilodalton (kDa) fragment and from this a final product of 33 kDa known as the C-terminal "core". These fragments remain attached to an N-terminal 10-kDa fragment. The 35-kDa–10-kDa complex is able to polymerize upon addition of KCl and $MgCl_2$, like intact actin, whereas the 33-kDa–10-kDa complex is not. The 35-kDa–10-kDa complex is here termed "split actin". In the rigor state, split actin binds to myosin subfragment 1 (S-1) strongly, with the same stoichiometry as intact actin. In the rigor state, split actin forms a carbodiimide-induced cross-linked product with S-1; the cross-linking sites on the split actin and on S-1 were proved to be the N-terminal 10-kDa fragment of split actin and the 20-kDa domain of S-1. There was no cross-linking between the 50-kDa domain of S-1 and the 10 kDa of actin. Therefore, the structure of the split actin–S-1 complex differs somewhat from that of the complex with intact actin. The cross-linking of split actin to S-1 causes superactivation of S-1 ATPase to approximately the same extent as does cross-linking of intact actin, whereas non-cross-linked split actin activates S-1 ATPase to a lesser extent. The N-terminus of the 35-kDa fragment was found to be residue 45 (Val-45) by amino acid sequence analysis; so there is no residue missing in split actin.

In 1976, Jacobson and Rosenbusch (1976) reported that chymotryptic or tryptic digestion of G-actin produces only one major fragment, viz., a C-terminal large "core" with a molecular weight of ca. 33000. In their paper, they reported that this fragment could neither polymerize nor activate myosin subfragment 1 (S-1)[1] ATPase activity. On the other hand, Johnson et al., (1979) reported that this fragment is able to polymerize and to activate myosin ATPase after treatment with urea and subsequent renaturation. In our previous paper (Konno, 1987), we added several new findings, viz., that the

† This work was supported by Grant CI-8 from the American Heart Association and by Grant HL-16683 from the USPHS.
‡ Career Investigator Fellow of the American Heart Association. Permanent address: Hokkaido University, Hakodate, Hokkaido, Japan 041.

[1] Abbreviations: EDC, 1-ethyl-3-[3-(dimethylamino)propyl]carbodiimide; Tes, 2-[[tris(hydroxymethyl)methyl]amino]ethanesulfonic acid; 1,5-IAEDANS, *N*-(iodoacetyl)-*N'*-(5-sulfo-1-naphthyl)ethylenediamine; $NaDodSO_4$, sodium dodecyl sulfate; DTT, dithiothreitol; kDa, kilodalton(s); PMSF, phenylmethanesulfonyl fluoride; 5-IAF, 5-(iodoacetamido)fluorescein; PAGE, polyacrylamide gel electrophoresis; S-1, myosin subfragment 1; EDTA, ethylenediaminetetraacetic acid; TLC, thin-layer chromatography.

0006-2960/87/0426-3582$01.50/0